AIP | Applied Physics Letters

Band offsets and carrier dynamics of type-II InAs/GaSb superlattice photodetectors studied by internal photoemission spectroscopy

Yan-Feng Lao, P. K. D. D. P. Pitigala, A. G. Unil Perera, E. Plis, S. S. Krishna, and Priyalal S. Wijewarnasuriya

Citation: Applied Physics Letters **103**, 181110 (2013); doi: 10.1063/1.4827881
View online: http://dx.doi.org/10.1063/1.4827881
View Table of Contents: http://scitation.aip.org/content/aip/journal/apl/103/18?ver=pdfcov
Published by the AIP Publishing

Band offsets and carrier dynamics of type-II InAs/GaSb superlattice photodetectors studied by internal photoemission spectroscopy

Yan-Feng Lao,[1] P. K. D. D. P. Pitigala,[1] A. G. Unil Perera,[1,a)] E. Plis,[2] S. S. Krishna,[2] and Priyalal S. Wijewarnasuriya[3]
[1]*Department of Physics and Astronomy, Georgia State University, Atlanta, Georgia 30303, USA*
[2]*Center for High Technology Materials, Department of Electrical and Computer Engineering, University of New Mexico, Albuquerque, New Mexico 87106, USA*
[3]*U.S. Army Research Laboratory, Adelphi, Maryland 20783, USA*

(Received 3 September 2013; accepted 16 October 2013; published online 30 October 2013)

We use internal photoemission spectroscopy to determine the conduction band offset of a type-II InAs/GaSb superlattice (T2SL) *p*B*p* photodetector to be 0.004 (±0.004) eV at 78 K, confirming its unipolar operation. It is also found that phonon-assisted hole transport through the B-region disables its two-color detection mode around 140 K. In addition, photoemission yield shows a reduction at about an energy of longitudinal-optical phonon above the threshold, confirming carrier-phonon scattering degradation on the photoresponse. These results may indicate a pathway for optimizing T2SL detectors in addition to current efforts in material growth, processing, substrate preparation, and device passivation. © *2013 AIP Publishing LLC*. [http://dx.doi.org/10.1063/1.4827881]

The type-II InAs/GaSb superlattice (T2SL) is considered as an alternate material to HgCdTe (MCT) and quantum wells for infrared (IR) photodetectors,[1] owing to its advantages of material stability, high uniformity, suppression of Auger processes,[2] and high electron effective mass.[3] Although optimum performance of T2SL detectors outperforming MCT detectors is theoretically predicated, the actual T2SL device is in part subject to limitation of Shockley-Read-Hall (SRH) recombination dominated carrier lifetime.[4,5] In addition to efforts in improving quantum efficiency, recent emphasis[6] was placed on the unipolar-barrier detectors to reduce dark currents.[7] The unipolar-barrier design, e.g., using the *p*B*p* architecture,[8] can readily realize multicolor detection, to meet requirements of applications in the third-generation IR imaging system.[1] Despite this promising characteristic, the ability of tuning the valence and conduction band (VB and CB) offsets to attain unipolar barriers is not straightforward.[6,9] Although detectors are experimentally demonstrated,[7,8] it is a necessity to shed more light on experimentally clarifying band offsets between the absorber and barrier.

In addition to multicolor detection, high-temperature operation is another characteristic of the third-generation IR photodetector.[1] In this Letter, we employ internal photoemission (IPE) spectroscopy to study T2SL unipolar-barrier detectors,[7] with the *p*B*p* (Ref. 8) and *p*B*i*B*n* (Ref. 10) architectures. IPE determines temperature-dependent band gaps of the absorbers, and nearly zero CB offset [0.004(±0.004) eV] for the two-color *p*B*p* design. Aside from this, we found that carrier-phonon coupling plays an important role in affecting the device performance. Although the VB offset between the absorber and barrier (B) is high [0.661 (±0.002) eV], inefficient blocking of holes by the B-region at about 140 K causes a change from the two-color detection mode to one-color mode. Therefore, the B-region should be designed to provide better control of the majority holes if high-temperature operation is desired. In addition to this, IPE spectroscopy also provides evidence of photoresponse degradation possibly due to carrier-phonon scatterings.

IPE spectroscopy is an attractive method[11–14] for studying the properties of materials and optical processes occurring at the interface of two materials. Although initial reports dated back more than four decades ago,[11] IPE remains attractive, in particular, with recent demonstration of its advantages in characterizing new material systems, such as graphene and oxide-based structures.[13,14] Previous applications of IPE mainly focused on bulk heterojunctions, for example, to obtain their barrier heights.[11] Its applicability to superlattice structures is not yet demonstrated.

IPE refers to such a case where carriers are photoexcited and transmit from one material to another by passing through an interface. Photoexcitation typically occurs in the absorber before photoemission. As for a *p*B*p* T2SL detector shown in Fig. 1(a) where two *p*-type InAs/GaSb T2SL absorbers responsible for mid/long-wave infrared (MWIR/LWIR) absorption are separated by a B-region consisting of an InAs/AlSb T2SL, different optical transitions can be resolved by switching the bias polarity, as shown in Fig. 1(b). Possible transitions include those occurring across the band gaps of the absorbers (I) and the B-region (II) and across the VB offset at the absorber/B-region interface (III), the latter two of which can be observed in the higher photon energy regime. This is shown in the quantum yield (Y) spectra plotted in Fig. 1(c). Y, defined as the number of collected photocarriers per incident photon, is proportional to the multiplication of spectral responsivity and photon energy.[12] Spectral response was measured by a Perkin-Elmer system 2000 Fourier transform infrared (FTIR) spectrometer. A commercial bolometer with known and flat sensitivity is used for background measurements and calibrating the responsivity, in order to eliminate the influence of light source and optical components on the spectral line shape.

Quantum yield can be generally described by the following expression:[12]

a)uperera@gsu.edu

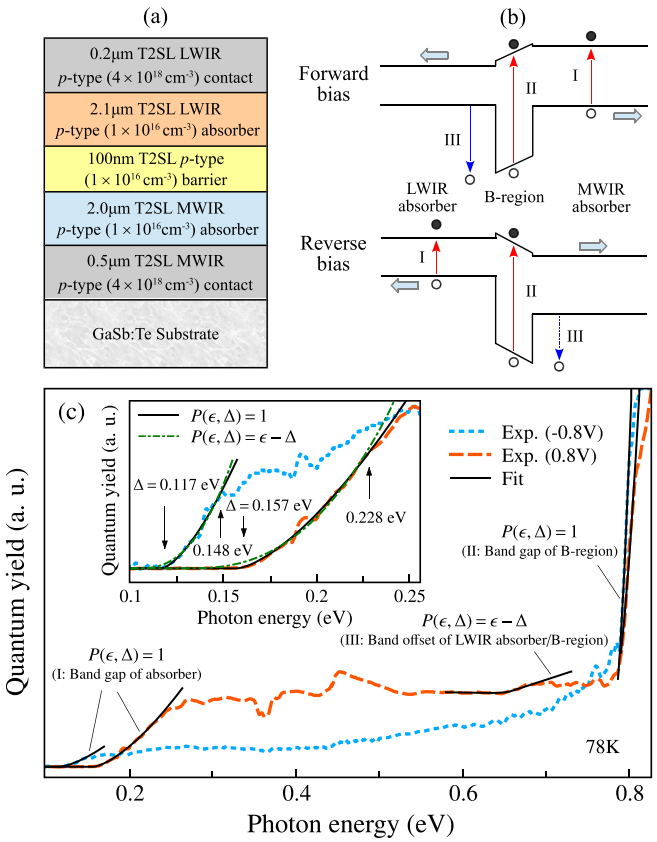

FIG. 1. (a) Schematic of a two-color type-II InAs/GaSb superlattice photodetector, based on a pBp architecture. The contact layers are the same as the absorbers except for the doping concentrations. (b) Band alignment under forward and reverse biases. The forward bias means a positive polarity applied on the top electrode of the detector. Shown are effective optical transitions contributing to photocurrents (depending on the bias polarity), including those across the band gaps (I and II) and band offset (III). The band offset transition under reverse (the vertical arrow with a dashed line) can theoretically occur, but is not observed in experiment. (c) The quantum yield spectra, along with IPE fittings (solid line) based on Eq. (1). The thresholds of optical transitions I–III can be obtained by fitting different energy regimes. Inset: comparison of fittings using different transmission probabilities.

$$Y(h\nu) = Y_0 + C_0 \int_{\Delta}^{\infty} \rho(\epsilon, h\nu)\, f(\epsilon, h\nu, E_f) \cdot P(\epsilon, \Delta)\, d\epsilon, \quad (1)$$

which takes into account two essential processes during IPE: photoexcitation in the absorber [described by an energy distribution function $\rho(\epsilon, h\nu)$] and the transmission of carriers over a barrier [described by a probability function of $P(\epsilon, \Delta)$]. C_0 is a constant independent of ϵ and $h\nu$. ϵ and $h\nu$ are the energies of photocarriers and incident photons, respectively. Δ is the photoemission threshold of a specific optical process under consideration such as the band gap of the absorber or the band offset at the absorber/B-region interface. The definition of Δ depends on the selection of an energy reference, which relies on the location of the Fermi level (E_f). For the present case (E_f in the band gap), the energy reference is selected at the VB edge. $f(\epsilon, h\nu, E_f)$ is the Fermi-Dirac distribution function, with the form of $[1 + e^{(\epsilon + E_f - h\nu)/kT}]^{-1}$ and $[1 + e^{(\epsilon - E_f - h\nu)/kT}]^{-1}$ for optical transitions across a band gap and a band offset, respectively. $\rho(\epsilon, h\nu)$ correlates with the joint density of states (JDOS). JDOS can be formalized by determining the absorption (α), since $\alpha \sim$ JDOS. In consideration of optical transitions between miniband states, the energy dependence of α can take a bulk-like formalism, as reported in Ref. 15, with the form of $\alpha(E) \sim (E - E_g)^n/E$, where n is determined to be 0.6. The denominator "E" is needed in order to incorporate an absorption tail. In the present work, such a tail is ignored as the tailing effect is negligible for the fittings, and thus $\rho(\epsilon, h\nu)$ takes the parabolic-band approximation of $(\epsilon - h\nu)^{1/2}$, which stands a valid formalism according to the results.

Fittings to quantum yield spectra in different near-threshold energy regimes were carried out, as shown in Fig. 1(c). In terms of Eq. (1), a background signal Y_0 should be subtracted, which can be due to thermionic emission[12] or contributions of the lower-energy transitions. Figure 2 plots various threshold energies obtained, showing nearly bias-independent behavior. A threshold energy corresponding to one specific transition is determined by the fact that the band offset has the value between the band gaps of absorbers and B-region. This determines the band gaps (average) of the LWIR and MWIR absorbers to be 0.117(±0.002) eV and 0.157(±0.001) eV, respectively, agreeing with the nominal values of 0.103 eV and 0.159 eV, respectively.[8] Based on the obtained VB offset [0.661 (±0.002) eV, as shown in the inset of Fig. 2], the CB offset at the LWIR absorber/B-region interface is determined as 0.004(±0.004) eV, close to the designed value (0.009 eV).[8] Such a small value should barely affect the transport of minority electrons.

It should be noted that photoemission probabilities should vary, in order to fit the band gap or band offset [see Fig. 1(c)]. With respect to IPE at an interface at which photocarriers need to overcome a potential barrier, $P(\epsilon, \Delta)$ equals $(\epsilon - \Delta)$ for $\epsilon \geq \Delta$ and 0 for $\epsilon < \Delta$,[12] according to an escape cone model.[16] It is apparent, however, that photocarriers excited in the MWIR/LWIR T2SL absorber can freely move towards the direction of photocurrents until being collected. This means 100% transmission probability. The IPE fittings using different $P(\epsilon, \Delta)$ plotted in Fig. 1(c) agree with the above operating mechanism. As shown in the inset of Fig. 1(c), the fitting using $P(\epsilon, \Delta) = (\epsilon - \Delta)$ leads to an incorrect spectral profile compared to $P(\epsilon, \Delta) = 1$, thus, not

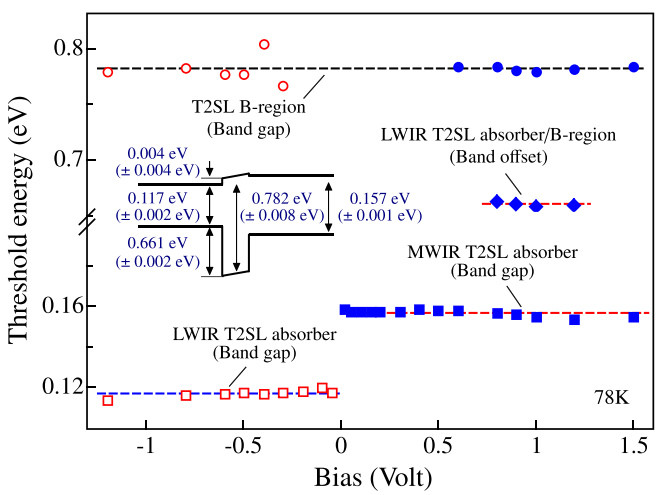

FIG. 2. The IPE determined threshold energies as a function of bias, corresponding to the band gaps of absorbers and the band offset at the LWIR absorber/B-region interface. The horizontal dashed lines are the averages of the data. Inset shows the band alignment.

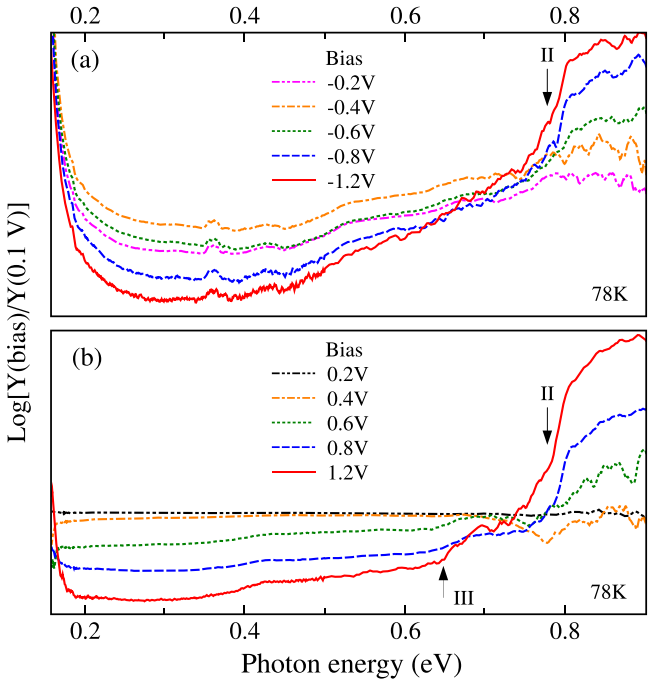

FIG. 3. Contrast yield spectra, defined as $Y(\text{bias})/Y(0.1\text{ V})$. The features related to transitions across the band offset (at the LWIR absorber/B-region interface, marked as III) are only observed at higher forward biases. The indicated II corresponds to the band gap of the B-region.

being able to explain the experimental data. The use of varied $P(\epsilon, \Delta)$ in consistence with optical processes under operation is a justification of the applicability of IPE spectroscopy to T2SL structures.

In comparison with the observations of photoemission thresholds resulting from transitions across band gaps, the band offset related threshold displays a relatively weak signature and only occurs at higher forward biases. A justification of the identified band-offset transitions not because of our experimental uncertainties is shown in the contrast yield spectra, defined as $Y(\text{bias})/Y(0.1\text{V})$, as shown in Fig. 3. For reverse bias, the effective transitions should occur across a band offset at the MWIR/absorber interface [Fig. 1(b)], at which, however, no apparent change in the slope of the yield spectra can be found (except for the band gap of the B-region, labeled as II). In contrast, an enhanced feature was observed at higher forward biases, attributed as correlated with the band offset at the LWIR absorber/B-region interface (labeled as III). The band-offset related optical transitions must occur within or between the VB minibands, thus leading to relatively weak absorption compared to that due to transitions across the band gap. This could be the reason of observations only at higher biases. The MWIR absorber has a deeper Fermi level in the band gap, and thus its absorption should be even less than the LWIR absorber, which may account for the unobservable feature of the band offset at reverse biases.

The temperature-dependent band gaps are shown in Fig. 4(a), which can be fitted by the empirical Varshni form,[17] $E_g(T) = E_g(0\text{K}) - \alpha T^2/(T+\beta)$. This gives $E_g(0\text{K}) = 0.166\text{eV}$, $\alpha = 0.53\,(\pm 0.08)$ meV/K, $\beta = 277\,(\pm 69)$ K for the MWIR absorber, and $E_g(0\text{K}) = 0.129$ eV, $\alpha = 0.30\,(\pm 0.07)$ meV/K, $\beta = 75\,(\pm 48)$ K for the LWIR absorber. Although band gaps can be measured by techniques such as photoluminescence, IPE spectroscopy has the advantage of characterizing detector devices consisting of multiple T2SL regions, each of which contributes to a luminescence peak, thus likely obscuring differentiation from one to another.

The confirmation of nearly zero CB offset between the absorber and B-region is evidence of high collection efficiency, as it does not block photoexcited minority electrons. In contrast, the B-region should be designed to provide a high VB offset between it and the absorber, and should fully block the majority holes. This is confirmed for operation at 78 K. However, although the VB offset [0.661 ($\pm$0.002) eV] is high enough to exclude any thermionic emission even at room temperature, it was observed that phonon-assisted transport of holes through the B-region from the MWIR absorber to the LWIR absorber deteriorates the two-color capability for temperatures above 140 K. As shown in Fig. 4(a), an abrupt increase in the threshold under reverse (negative) biases occurs at about 140 K. This means that the detector only displays the response characteristic of the MWIR absorber for both forward (positive) and reverse biases. The only possibility for this to occur is the majority holes in the MWIR absorber bypassing the B-region. It can be seen from Fig. 4(a) that the photoemission threshold obtained at high temperatures and negative biases is higher than the band gap of the MWIR absorber by an amount of 26 ± 5 meV, nearly the

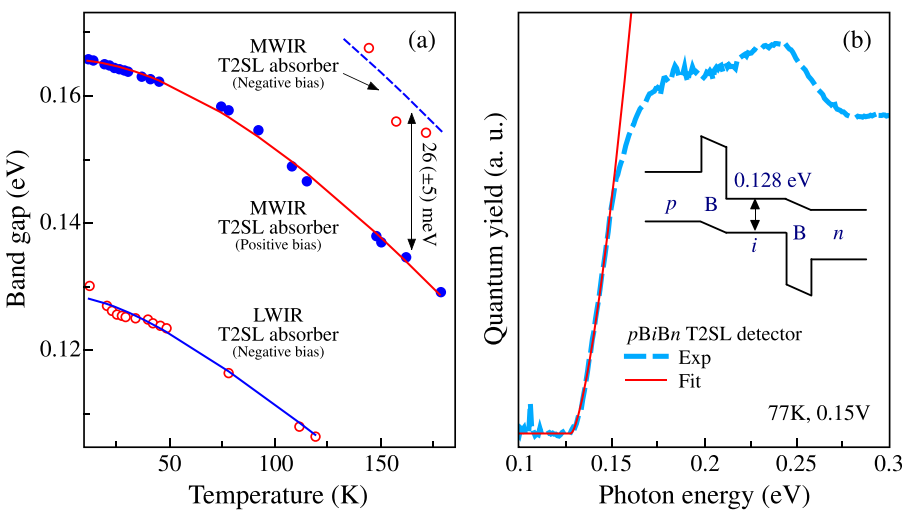

FIG. 4. (a) The IPE determined band gaps of absorbers (scatter points) as a function of temperature, which are fitted to the empirical Varshni form (solid lines).[17] (b) IPE fitting to the quantum yield spectrum of a *p*B*i*B*n* detector, giving the band gap of the *i*-absorber as 0.128 eV. Inset shows the band alignment.

energy of the longitudinal-optical (LO, $\sim$ 30 meV) phonon. This points to the LO phonon-emission assisted tunneling[18] as a possible cause. At relatively high temperatures, the distribution of holes is expanded into higher energy states, and thus some of them lie in the leaky window of tunnelling.[18] Consequently, a higher passing probability through the B-region is expected, giving rise to response due to the MWIR absorber.

Contrary to the dominant response of the MWIR absorber, the response of the LWIR absorber is weaker and not observable at high temperatures. Analysis of the IPE results allows us to deduce a carrier-phonon scattering mechanism which is responsible for the photoemission yield reduction.[11] As shown in the inset of Fig. 1(c), for the negative bias operation (the LWIR absorber is active), experimental yield drops below the fitting curve at photon energy 31 meV above the threshold. The absorption of T2SLs display a profile, but with a drop point nearly 200 meV above the band gap.[19] It is understandable that significant scattering events occur when the kinetic energies of carriers are greater than the energy of LO phonon. Scatterings will redirect the moving direction of holes or decrease their energies, thus causing a reduction in the escape probability. This assertion is partially supported by the independence of the dropping point on the applied bias. In contrast, the yield drop point is 71 meV higher than the threshold for positive bias operation, and thus no apparent scattering degradation can be confirmed for the MWIR absorber. The carrier-phonon scattering mechanism thus accounts for the lower responsivity of the LWIR absorber than that of the MWIR absorber. Optimization to reduce the carrier-phonon scattering effects provides an alternative pathway to improve the performance of the T2SL detectors in addition to current efforts in material growth, processing, substrate preparation, and device passivation.[1]

The IPE method is also extended to fit the quantum yield spectrum of a *p*B*i*B*n* T2SL detector,[10] as shown in Fig. 4(b), where the absorber uses an *i*-type instead of *p* in the *p*B*p* detector. As no barrier appears for the transport of minority electrons and holes, a 100% transmission probability was used. A band gap of 0.128 eV is obtained by fitting the near-threshold regime. The agreement between the fitting and experimental spectrum is good, which further confirms the capability of the IPE method for characterizing T2SLs.

To conclude, we presented IPE studies on InAs/GaSb T2SL photodetectors using *p*B*p* and *p*B*i*B*n* architectures. The band gaps of photon absorbers and their temperature dependence are determined by IPE spectroscopy, based on fittings to the quantum yield near-threshold regimes. IPE simultaneously determines the VB and CB band offsets (for the *p*B*p* structure) at the LWIR absorber/B-region interface as 0.661 ($\pm$0.002) eV and 0.004 ($\pm$0.004) eV, respectively. IPE spectroscopy also illustrates the effect of carrier-phonon scatterings on the degradation of the LWIR photoresponse at 78 K. Additionally, LO phonon-emission assisted tunneling is considered as a cause for the failure of two-color detection in the *p*B*p* detector at about 140 K.

This work was supported in part by the U.S. Army Research Office under Grant No. W911NF-12-2-0035 monitored by Dr. William W. Clark, and in part by the U.S. National Science Foundation under Grant No. ECCS-1232184.

[1]A. Rogalski, J. Antoszewski, and L. Faraone, J. Appl. Phys. **105**, 091101 (2009).
[2]C. H. Grein, P. M. Young, M. E. Flatté, and H. Ehrenreich, J. Appl. Phys. **78**, 7143 (1995).
[3]F. Fuchs, E. Ahlswede, U. Weimar, W. Pletschen, J. Schmitz, M. Hartung, B. Jager, and F. Szmulowicz, Appl. Phys. Lett. **73**, 3760 (1998).
[4]B. C. Connelly, G. D. Metcalfe, H. Shen, and M. Wraback, Appl. Phys. Lett. **97**, 251117 (2010).
[5]D. Donetsky, G. Belenky, S. Svensson, and S. Suchalkin, Appl. Phys. Lett. **97**, 052108 (2010).
[6]D. Z.-Y. Ting, A. Soibel, L. Hoglund, J. Nguyen, C. J. Hill, A. Khoshakhlagh, and S. D. Gunapala, *Advances in Infrared Photodetectors (Semiconductors and Semimetal Series)*, edited by S. D. Gunapala, D. Rhiger, and C. Jagadish (Elsevier, 2011), Vol. 84, Chap. 1, pp. 1–57.
[7]B.-M. Nguyen, S. Bogdanov, S. A. Pour, and M. Razeghi, Appl. Phys. Lett. **95**, 183502 (2009).
[8]E. Plis, S. Krishna, N. Gautam, S. Myers, and S. Krishna, IEEE Photonics J. **3**, 234 (2011).
[9]D. Z.-Y. Ting, C. J. Hill, A. Soibel, S. A. Keo, J. M. Mumolo, J. Nguyen, and S. D. Gunapala, Appl. Phys. Lett. **95**, 023508 (2009).
[10]E. A. DeCuir, N. Gautam, G. P. Meissner, P. Wijewarnasuriya, S. Krishna, N. K. Dhar, T. G. Bramhall, R. E. Welser, and A. K. Sood, Proc. SPIE **8512**, 85120N (2012).
[11]V. Afanas'ev, *Internal Photoemission Spectroscopy: Principles and Applications* (Elsevier Science, 2010).
[12]Y.-F. Lao and A. G. U. Perera, Phys. Rev. B **86**, 195315 (2012).
[13]R. Yan, Q. Zhang, W. Li, I. Calizo, T. Shen, C. A. Richter, A. R. Hight-Walker, X. Liang, A. Seabaugh, D. Jena, H. G. Xing, D. J. Gundlach, and N. V. Nguyen, Appl. Phys. Lett. **101**, 022105 (2012).
[14]Y. Hikita, M. Kawamura, C. Bell, and H. Y. Hwang, Appl. Phys. Lett. **98**, 192103 (2011).
[15]G. Ariyawansa, M. Grupen, J. M. Duran, J. E. Scheihing, T. R. Nelson, and M. T. Eismann, J. Appl. Phys. **111**, 073107 (2012).
[16]R. Williams, "Injection Phenomena," in *Semiconductors and Semimetals*, edited by R. Willardson and A. Beer (Academic Press, New York, 1970), Chap. 2.
[17]I. Vurgaftman, J. R. Meyer, and L. R. Ram-Mohan, J. Appl. Phys. **89**, 5815 (2001).
[18]M. V. Kisin, M. A. Stroscio, G. Belenky, and S. Luryi, Appl. Phys. Lett. **80**, 2174 (2002).
[19]L. L. Li, W. Xu, and F. M. Peeters, Phys. Rev. B **82**, 235422 (2010).